

<https://doi.org/10.1038/s44182-025-00056-x>

Biohybrid living robotics: A comprehensive review of recent advances, technological innovation, and future prospects

Ali Garmroudi¹, Md Abdul Kader Tushar¹, Chang Liu¹ & Zhengwei Li^{1,2}✉



Biohybrid robotics combines living components with synthetic materials to create adaptable, responsive robots. This review focuses on bottom-up, tissue-based biohybrid robots-Walkers, Swimmers, Grippers, Pumps, and emerging eBiobots, which use living actuators for various tasks. We explore their design, innovations, and applications, and highlight recent advances in intelligent eBiobots integrating neurons, muscles, biomaterials, and microelectronics. Future directions emphasize interdisciplinary progress toward intelligent biomachines for transformative applications in health, medicine, environmental monitoring and beyond.

Robotics is currently undergoing a deep revolution in both its design principles and constitutive elements, to effectively tackle the challenges of today's world^{1–4}. Biohybrid robotics (or 'Bio-bots') represents an exciting paradigm, which have emerged through the integration of living cells or tissues with engineered flexible structures (Fig. 1). There are two approaches for biobot fabrication: bottom-up, and top-down^{5,6}. The bottom-up approach contains fabrication of structures, cell culture for the contraction unit, and the integration of the biobots' different components. The top-down approach refers to designing and constructing robots starting from the higher-level functional goals and systems, such as the overall behavior and task the robot is intended to perform, and then working down to the details of its components, including the biological components. The main focus of this work is allocated to bottom-up systems. We therefore emphasize tissue-engineered actuators (e.g., cardiac or skeletal muscle, insect tissue) integrated into soft robotic platforms. Biohybrids based on whole organisms, single-celled microbes, or DNA nanostructures are beyond our scope.

Traditional robotics is often constrained by rigid structures and limited adaptability. To fix this, soft robots have been created composing of soft materials like elastomeric polymers which were inspired by animals with no hard internal skeletons. One of which is quadrupedal robot capable of complex motions using no sensors and five actuators⁷. While soft robots use soft materials for their structure which is similar to biobots, they typically rely on external power sources, and have limited biocompatibility, while the biobots leverage the dynamic, adaptive nature of biological system integrated with engineered platforms. By directly combining the living components such as cardiomyocytes^{8–15}, skeletal muscles^{16–20}, nerve cells¹⁸, or

insect Dorsal Vessel Tissue (DVT)^{21–23}, biohybrid robots have gained unique abilities to perform lifelike movements, sense their environment, and respond to dynamic stimuli and perform different task like grabbing or even weight lifting²⁴. Contractility is an essential electrophysiological feature of muscle cells. Muscle cell contraction is regulated with excitation-contraction (EC) coupling process. First, an action potential (AP) is activated in the cell membrane which then continues by a series of events that relate the AP-mediated excitation to contractility of muscle cells. The most crucial step in EC coupling process is Ca^{2+} ion balance over the membrane of the cell. The chemical gradients of Ca^{2+} ions in the cell membrane are crucial for the propagation of APs. Aps, however, spontaneously propagate in cardiac cells while a nervous stimulus via neuromuscular junctions is required to activate skeletal muscle cells. Electrical stimulation aims to recreate such electrical signals for skeletal muscle or cardiac cells *in vitro* to generate APs²⁵. These systems also provide valuable insights into the fundamental design principles of biological systems in controlled *in-vitro* settings, which can then be applied to artificial designs, leading to unprecedented performance and innovative applications^{26,27}.

Pioneering studies have utilized muscle cells and tissue constructs as living actuators. An interesting work has even gone so far to train the muscle tissue through weightlifting of the *in-vitro* muscle tissue²⁴. These living actuators are to enable locomotions in various types of biobots including walking biobots^{9,16,17,28,29}, swimming biobots^{10–12,18}, gripping biobots^{19,20,23}, pump biobots^{30,31}, and even biobots that are detected by light^{13–15}. Walking biobots, powered by engineered muscle cells, cardiac cells, or DVT are designed to mimic natural walking or crawling locomotion of worms (caterpillars)¹⁵ and other walking species¹⁶. Swimming biobots, often driven

¹Department of Biomedical Engineering, Cullen College of Engineering, University of Houston, Houston, TX, USA. ²Department of Biomedical Sciences, The Tilman J. Fertitta Family College of Medicine, University of Houston, Houston, TX, USA. ✉e-mail: zli65@central.uh.edu

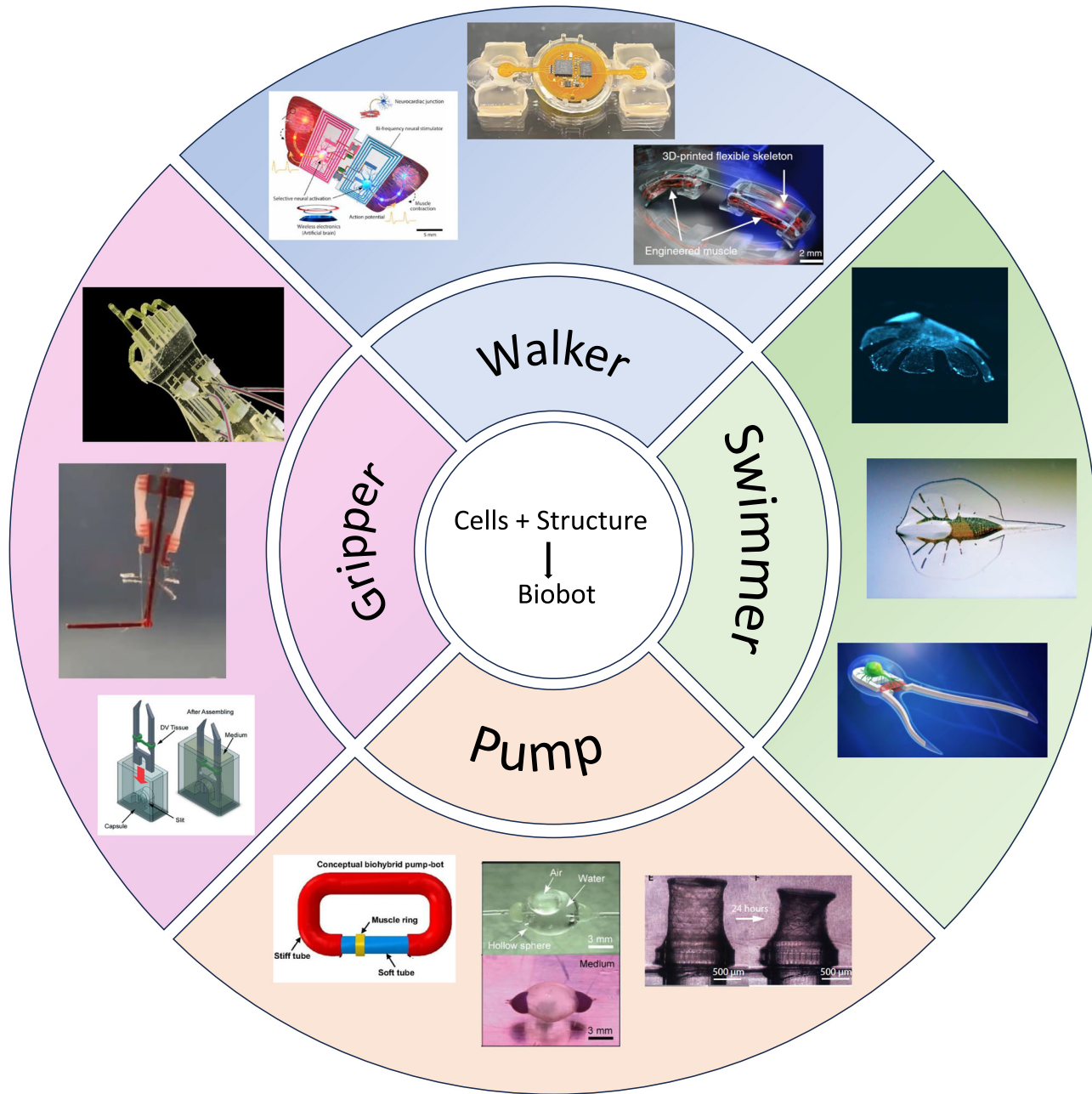


Fig. 1 | Biobot classification based on locomotion. Biohybrid robots can be classified into Walker, Swimmer, Gripper, and Pump, with e-biobots being the future of the field as subset of walkers, and swimmers^{41,42}. Reprinted with permission from AAAS. Walker biobots mimic a worm-like crawling locomotion^{28,88}. Reprinted with permission from AIP Publishing and Springer Nature respectively. The swimming biobots mimic the aquatic life swimming motion^{10,12} (<https://scitechdaily.com/microscopic-biohybrid-robots-propelled-by-muscles-nerves-built-by-researchers/>, <https://www.popsci.com/soft-robotic-stingray/>). Reprinted with permission from

American Association for the Advancement of Science. Gripper biobots utilize contraction of cells to manipulate objects^{19,21,73}. Reprinted with permission from American Association for the Advancement of Science, Mary Ann Liebert, Inc, and American Association for the Advancement of Science respectively. Pump bots utilize the contraction of the muscles for manipulating objects and perform bending motions^{34,35,75}. Reprinted with permission from Royal Society of Chemistry, PNAS, and AAAS respectively.

by cardiac cells^{10–12} or skeletal muscle cells¹⁸, are capable of functioning and navigating in both low-Reynolds^{11,18} (environments in which viscous forces dominate inertial forces, causing smooth and laminar flow) and high-Reynolds^{10,12} environments (environments in which inertial forces are dominant, causing turbulent flow), holding promising applications in fields such as biomedicine, environmental monitoring^{32,33}, and targeted drug delivery. Gripping biobots utilize contractile tissues to perform tasks such as picking up or holding objects and manipulate these objects with flexibility and precision, making them ideal for tasks requiring delicate handling. Pump bots try to mimic the function of heart and pumps liquid by repetitive

contractions and relaxations of the contracting unit^{34,35}. Other than these, some bots are also capable of dynamically changing the color of their platform by altering the nanophotonic structures on its surface. This novel approach allows for real-time color modulation, driven by the interaction between biological components and engineered nanostructures, expanding potential applications in bio-sensing and signaling technologies. For example, morpho butterflies with parallel periodic nanoridges on the surface of their wings manipulate the transmission of photons in their photonic bandgap^{36–40}. The photonic bandgap which is the range of light wavelengths that are not absorbed by the surface structure but reflected from it, causes

this color variation. By assembling cardiac tissues on the morpho butterfly wings, the contraction of this biological component which is aligned with the nanoridges structure of morpho butterfly wings, bends the wings. Hence, it creates a novel biological sensor detectable without complex equipment¹³.

More recently, a new subclass of electronic biohybrid robotics (“eBiobots”) has emerged, through the unusual combination of bioengineered muscle tissues, motor neurons, as well as advanced wireless optoelectronics. One groundbreaking work is the hybrid bioelectronic robots (eBiobots) equipped with battery-free and microinorganic light-emitting diodes for wireless control and real-time communication. The design enables remote control of the coordinated functions such as walking, turning, plowing, and transporting objects, both individually and in collective formations. This groundbreaking work represents a significant step forward in the development of remotely controlled miniature biobots with huge potential applications in medicine, sensing and environmental monitoring. Another pioneer example is the wirelessly steerable bioelectronic neuromuscular robots, a frequency multiplexing wireless system, functioning as an artificial brain, which was used to stimulate the motor neurons, which in turn activated the cardiac muscle cells. These biohybrid electronic systems pave a new pathway toward creating a class of next-generation intelligent biomachines and systems capable of adaptive motor control, learning, and higher-order intelligence^{41,42}.

This review article begins with an overview of biohybrid approaches for the development of biobots, which are categorized into four major types: Walkers, Swimmers, Grippers, and pump bots. Each category is designed to perform specific functions by harnessing biological processes in combination with synthetic components, as summarized in Fig. 1. This functional taxonomy highlights distinct locomotor and manipulative modalities of biohybrid robots, enabling systematic comparisons across systems. Unlike other classification schemes that focus on actuation source⁴³ or scale⁴⁴, our categories emphasize functional roles and design parallels. The following sections discuss the progresses, innovations, and potential applications within each category. Finally, the article discusses the challenges and future directions, emphasizing the convergence of interdisciplinary efforts that leverage technological innovations in materials science, bioengineering, and artificial intelligence to build the next generation of intelligent biohybrid machines. Recent reviews^{43–46} have addressed complementary aspects of biohybrid robotics. For example, Sun et al.⁴⁵ focused on cell-based actuators, control methods, and biomedical applications; Mestre et al.⁴⁴ highlighted developments from the nano- to macroscale; and Li & Takeuchi⁴⁶ detailed contraction models and control techniques. Webster-Wood et al.⁴³ further provided historical context across microorganisms, cyborgs, and tissue-based robots. These works complement our analysis, but our focus on functional categories and bottom-up design offers a new perspective on the interrelationships among biohybrid robot classes.

Biohybrid motile bots

Biohybrid motile robots integrate living cells with artificial structures to achieve desired locomotion and perform various tasks. These robots can exhibit diverse movement modalities, including walking, crawling, swimming, and bending. Early breakthroughs in the field, such as the Muscular Thin Films (MTFs) that demonstrated how cardiomyocytes on a flexible structure could enable complex behaviors like walking and crawling (Fig. 2A)⁸. Since then, advances in biohybrid robotics have focused on enhancing movement efficiency, control, and adaptability through technical innovations, such as the introduction of advanced microelectronics into biorobotic systems.

Walkers

Walking biobots are inspired by the locomotion of various species, such as worms, caterpillars¹⁵, crabs⁴⁷, and other crawling/walking organisms⁹. Inspired by the movement of worms, some researchers developed crawling biorobotic prototype⁹, while others designed leg-based locomotion systems mimicking the walking creatures^{16,28,29}. A key feature of these systems is the

asymmetry of the walking surface, which generates friction in one or multiple directions to facilitate movement. The first major contribution in this area was created by a simple yet innovative structure that moved forward with each contraction (systole) and relaxation (diastole) of the cells, achieving a speed of 8 mm/min (Fig. 2A). The researchers used an electric field at a frequency of 1 Hz to stimulate cell contraction, enabling this movement⁸.

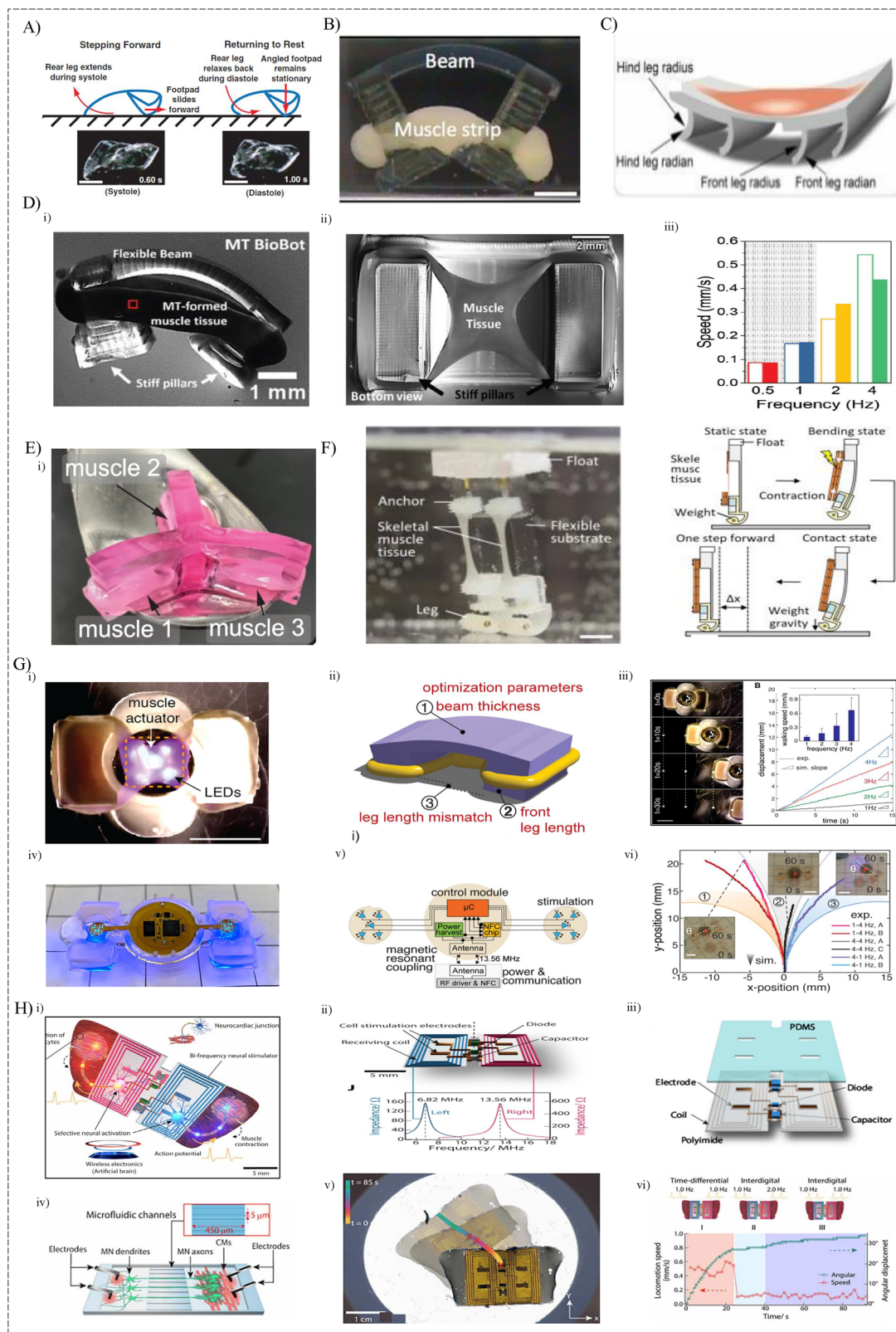
In 2012, a novel walking biobots using a cardiac cell sheet as the contracting unit was reported, coupled with Polyethylene Glycol Diacrylate (PEGDA) hydrogel as the bending structure along and a base of a PEGDA hydrogel with different molecular weight. The base in this setup was the basis of asymmetry facilitating the movement of the system, achieving velocity of 236 $\mu\text{m/s}$ ⁹.

The researchers later innovated further by designing a new structure, featuring a contracting skeletal muscle strip controlled by real-time electrical stimulation (bipolar pulse train: 20 V amplitude, 50 ms pulse length) (Fig. 2B). This system reached a maximum speed of 156 $\mu\text{m/s}$ (or 1.5 body lengths per minute). When tested at different electrical stimulation frequencies (1–4 Hz), walking speed increased with higher frequencies. This is understandable since the frequency of stimulation correlates with the number of contractions of the actuation units integrated in the biobots, i.e. the system makes the movement in a relatively shorter period of time, hence, increasing the speed. The use of the bioengineered 3D skeletal muscle tissues that are made of C2C12 myoblast cell lines, allows for external control of muscle contraction and biobot movement⁹. A more recent work took advantage of gracilis minor tissue from bullfrog as the contracting unit which was placed on top of the surface of the walker biobot. This muscle was chosen for its high contractile force (~4.4 N), and faster contraction compared to its counterparts (Fig. 2C)⁴⁸. Additionally, a light-responsive skeletal muscle bioactuator made of optogenetic C2C12 myoblasts was developed, which can generate significant active tension when stimulated by a noninvasive optical signal. This innovation resulted in a velocity of 310 $\mu\text{m/s}$ (1.3 body lengths/min) and a rotational speed of 120 degrees/min. The introduction of muscle rings further enhanced the system’s speed (Fig. 2D-i). A comparison between electrical and optogenetic stimulation showed minimal differences in speed (Fig. 2D-iii)⁴⁹. There is generally very small difference between the velocity of biobots when electrically stimulated compared to optically stimulated. Further improvement, including multi-leg designs, enabled the biobot to move in multiple directions (Fig. 2E)²⁹. Increasing tissue force output is crucial for enhancing the performance of biohybrid robots⁵⁰. Another work advanced this concept by elongating C2C12 myoblasts, adjusting structure geometry and mechanical properties, and using stiffer structures. These innovations increased force per stroke threefold, achieving speeds >0.5 mm/s at a frequency of 4 Hz (>2.3 body lengths/min) (Fig. 2E-iii)⁴⁹.

Inspired by caterpillar movement, a research work, developed a multi-legged, caterpillar-like crawling biohybrid robot. This design used asymmetric claws on its surface to generate movement, with the biobot bending along its length during contraction and straightening during relaxation. This work also tested the effects of different drugs on the biobot’s velocity showcasing that the biobot can reach the maximum speed when the length of claws are between 160–200 μm . Crawling speed was influenced by both the tilt and length of the claws, initially increasing with greater claw length and tilt. However, beyond a certain point, further increases in these parameters resulted in a significant decrease in speed¹⁵.

Another crawling system, utilized insect dorsal vessel tissue (DVT) as the contracting unit. By positioning the DVT closer to one end of the structure, asymmetry was created, causing the biobot to move toward that end. While the system was designed for unidirectional movement, slight shifts in direction were observed, causing small changes in the biobot’s position along the y-axis²².

Stepping out of the normal pillar-based walking biobots were the contracting unit usually encircles around the pillars, a novel model of walking biobot which was based upon earlier work of gripping biobots (other class of biobots)⁵¹ was developed where the skeletal muscle tissue is held by



an anchor and bends the flexible structure (Fig. 2F-i)). By each contraction and relaxation, the system moves “one step” forward (Fig. 2F-ii)).

eBiobot walkers

Biohybrid electronic robots (eBiobots) integrate electronic products with biological components to enable precise, electrically controlled

movement. By incorporating microelectronics, eBiobots can respond to electrical stimuli, allowing real-time control over their movement and function. This novel approach by the unusual combination of technology and biology paves the way for next-generation intelligent biobots with wide range of applications in biomedicine and environmental monitoring.

Fig. 2 | Walker biobots. **A** Muscular thin films. A layer of cardiac fibers on hydrogel that will contract and cause the crawling movement of the system⁸. Reprinted with permission from AAAS. **B** the setup of a walking system illustrating the structure design and muscle strip's location on the structure. The system is shown in contracted state¹⁶. Reprinted with permission from PNAS. **C** Walker biobot using gracilis minor muscle tissue driven from a bullfrog⁴⁸. Reprinted with permission from Sensors and Actuators B: Chemical. **D** **i.** Myotube muscle tissue-based walking biobot with aligned cells along the contracting direction. **ii.** Bottom view of the same design showing the geometry of the muscle tissue. **iii.** difference in velocity in a range of stimulating frequencies⁴⁹. Reprinted with permission from John Wiley and Sons. **E** other designs of walking biobots with pillars and muscle rings attached to them to enhance mobility in different directions²⁸. Reprinted with permission from Wiley-VCH GmbH. **F** **i.** Novel walking biobot with bipedal design floating in the medium. **ii.** Walking mechanism of the bipedal walking biobot⁵². Reprinted with permission

from Elsevier. **G** Biohybrid Electronic Robot. **(i)** eBiobot illuminated by five μ -ILEDs. **(ii)** Two unevenly sized legs joined by a narrow connecting beam. **(iii)** The moving capabilities of the eBiobot, powered by 10-W radio frequency and five μ -ILEDs. **(iv)** Updated Bipedal eBiobot. **(v)** Schematic of the wireless control framework including μ C and NFC Chip. **(vi)** eBiobot's turning directions and optical stimulations⁴¹. Reprinted with permission from AAAS. **H** Neuromuscular Electronic Robots. **(i)** Particular innervation of CMs by frequency multiplexed wireless device. **(ii)** Structure of Electronic Complex with Left and right coils' resonant frequencies. **(iii)** Fabrication process of wireless bioelectronic device. **(iv)** Schematic of a microfluidic device to test neurocardiac junctions. **(v)** Locomotion characteristics of Biohybrid Neuromuscular Robot **(vi)** Locomotion speed and angular displacement at various transmission signals. Scale bars, 5 mm [G (i and iii), H(i)], 1 cm [H(v)]⁴². Reprinted with permission from AAAS.

One notable example is the wireless biohybrid electronic robot (wireless eBiobot), which integrates skeletal muscle actuators with wireless bioelectronic devices for remote movement control⁴¹. The system incorporates three key components: bioengineered living optogenetic muscle actuator, wireless and battery-free optoelectronics (including μ -ILEDs), and a 3D-printed hydrogel skeleton (Fig. 2G-i). Muscle tissues are placed on a hydrogel structure and the electronic device stimulates the tissues using micro-inorganic light-emitting diodes (μ -ILED) which induce cyclical muscle contractions. These contractions cause the structure to bend, leading to robot movement. The robot is powered wirelessly via a 13.56 MHz Radio Frequency (RF) power provider system, which uses magnetic resonance to transfer power from the transmission antenna to the device's antennas. Stimulation frequency and pulse width can be adjusted using the RF amplitude modulation techniques, managed by a computer. Here, skeletal muscle tissue developed on a 3D-printed hydrogel structure, and this structure was intended to contain the optoelectronic device in the middle. Figure 2G-ii shows a length discrepancy between the front and back legs, making it possible to move. Frequency, surface friction, and μ -ILED structure are responsible for walking speed, and the speed changes when frequency increases or decreases (Fig. 2G-iii). The eBiobot's performance, such as walking speed, can be optimized by altering factors like frequency, surface friction, and μ -ILED structure. When triggered at 4 Hz (frequency), 50 ms (pulse width), and 10 W (RF power), the eBiobot reached a top walking speed of 0.83 mm/s (3.56 body lengths/min). To improve mobility, eBiobot was upgraded (Fig. 2G-iv) with a bipedal structure featuring two muscle actuators controlled by a central microcontroller (μ C). This eBiobot offers precise movement control by initiating muscle contractions at different points on the same robot. In addition, using Near Field Communication (NFC) chipsets, each robot could be precisely targeted, permitting coordinated operation across multiple eBiobot units within the sage antenna cage (Fig. 2G-v). Three essential movements (Fig. 2G-vi) were achieved under three different stimulation patterns (left turn, 1Hz-4Hz; straight, 4Hz-4Hz; right turn, 4Hz-1Hz). The eBiobot demonstrated durable bidirectional and forward movement remotely by differential and symmetrical excitation.

Neuromuscular Electronic Robot, which connects the Motor Nervous System of cardiac muscle with a biohybrid electronic robot to mimic cardiac muscle activity and regulate neural motion⁴². As an alternative to chemical synapses, electrical synapses of human-induced pluripotent stem cells generated motor neurons (iPSC-MNs) and cardiomyocytes (iPSC-CMs), were merged into the bioelectronic robot (Fig. 2H-i). These electrical synapses, with the help of gap junctions and quicker bilateral signaling, establish connections between various kinds of cells. To design the neuromuscular electronic robot, the researchers first created these neuro-cardiac junctions and then integrated them into a wireless flexible electronic module. The wireless module functions as an artificial brain and guides targeted neural stimulation that triggers the fin movements of the robot by transferring signals between iPSC-MNs to iPSC-CMs through the electrical synapse. Electrically excited iPSC-MNs can activate iPSC-CMs, enabling the

sensory-motor capabilities of CM-based biohybrid systems. The frequency multiplexing system makes targeted neural stimulation possible. The device delivers two different modulated signals featuring frequency, and pulse width at 13.56 MHz and 6.82 MHz (Fig. 2H-ii), which enables independent control of the robot's locomotion (left and right fins). Two resonant coils receive these signals via magnetic coupling that produces voltages and activates iPSC-MN tissues placed on two different resonant coils. Figure 2H-iii, iv shows fabrication process and core electronic components to prepare this device. Furthermore, the left and right fin-flapping speed and synchronization were independently controllable by modifying transmitted signal configurations. To monitor its locomotion performance, the device was placed within 25 mm of a Petri dish (Fig. 2H-v) surrounded by excitation coils. The neuromuscular robot achieved effective forward locomotion through alternate flapping of its left and right wings (speed, ~0.57 mm/s at Time-differential Mode-I). However, when the fins flapped simultaneously, movement speed decreased to around 0.11 mm/s (Interdigital Mode-I), showcasing the importance of precise timing and control in achieving effective locomotion (Fig. 2H-vi)⁴².

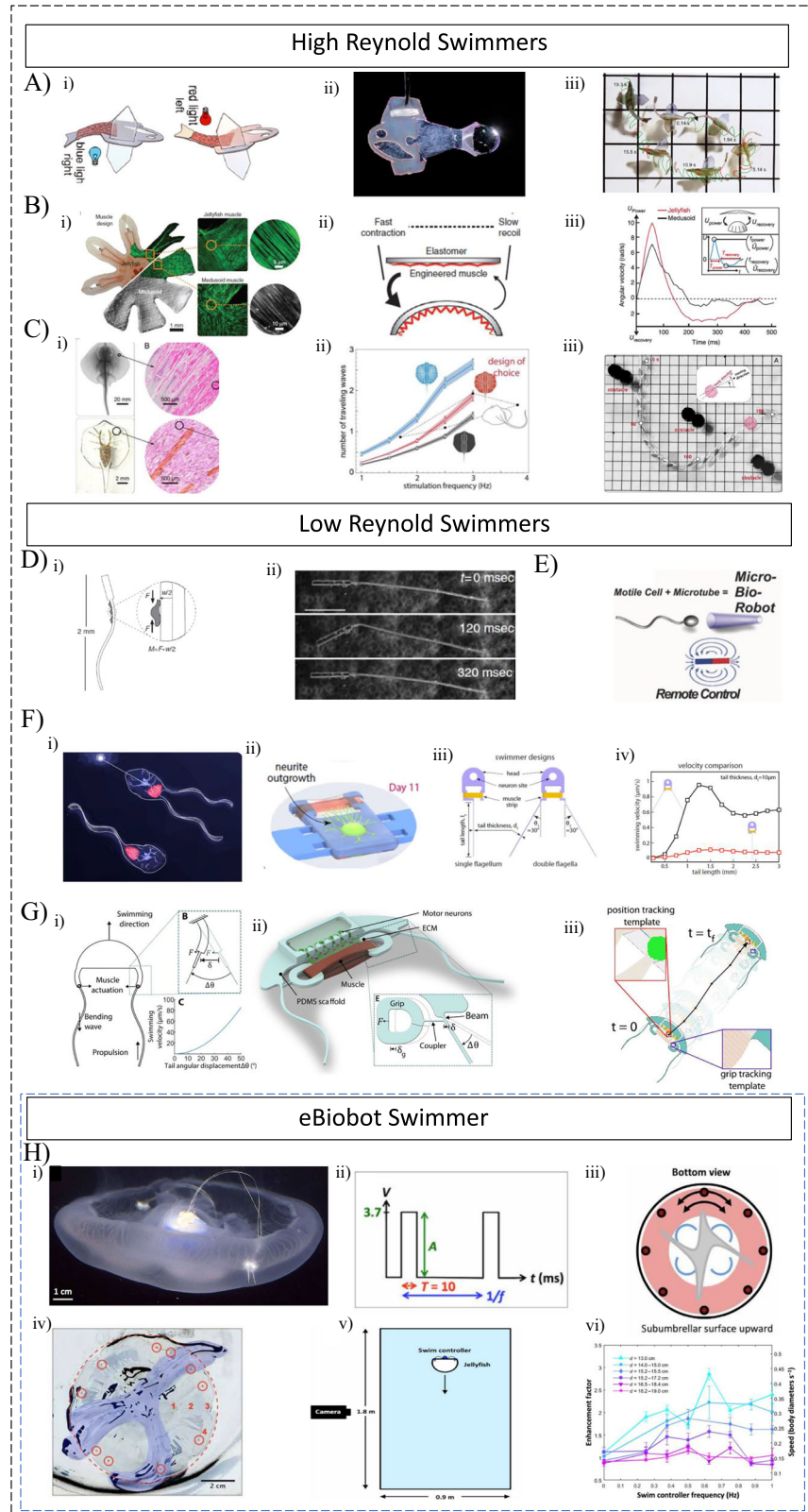
In addition to these two eBiobots, some other electronic biohybrid robots have also demonstrated walking capabilities. A maneuverable walking biological robot was introduced to exhibit robust straight motion as well as turning³². This dual-ring biobot is made up of two independent muscle actuators and a four-legged, asymmetric structure in the fore/aft direction. The robot can move because it has various muscles integrated into its body architecture, as well as differential electrical stimulation.

These systems are laying the groundwork for innovations in biomedicine, such as targeted drug delivery and tissue repair, and environmental monitoring, where they dynamically adapt to and respond to ecological changes.

Swimmers

Swimming biobots are designed to mimic the locomotion of aquatic organisms, propelled by rhythmic muscle contractions through fluid environments. Swimming biobots can be broadly classified as high Reynolds number swimmers and low Reynolds number swimmers, based on the fluid dynamics (Fig. 3). In the high Reynolds domain, a research work built a swimming biobot using DVT as the actuation unit. The biobot moved by bending in response to the rhythmic contraction and relaxation of the DVT, supported by a flexible polydimethylsiloxane (PDMS) structure, achieving a speed of 11.7 μ m/s, though falling short of their theoretical estimate of 44.7 μ m/s⁵³. Another team created a fish-like biobot, in which cardiac cells on opposite sides of the structure allowed directional control by using light: blue light stimulated one side, and red light activated the other, enabling bidirectional movement (Fig. 3A-i, ii)⁵⁴. In a prior study, a jellyfish-inspired medusoid biobot was developed that mimicked the jellyfish's pulsatile swimming, achieving efficient angular velocity through electrically stimulated contractions (Fig. 3B)¹⁰. This design was further validated in real-world tests in Massachusetts coastal waters, where the biohybrid jellyfish reached speeds of 6.6 cm/s.

Fig. 3 | Swimmer biobots. High Reynold Swimmers. **A** i, ii. a fish-like biobot with muscle tissue on both sides of the biobot enhancing the locomotion and directionality of the system. ii. The movement results of the system showing great locomotive abilities of the setup⁵⁴. Reprinted with permission from AAAS. **B** The Medusoid; The biobot inspired by jellyfish. i. comparison of muscle alignment and form of actual jellyfish (top) and the fabricated jellyfish biobot which is called medusoid. The microscopic results of the cell alignment show great similarities between the two. ii. The moving mechanism of the medusoid with fast contractions and slow recoil making it move upwards. iii. The angular velocity comparison between the jellyfish and the fabricated medusoid showing better functionality of the medusoid in long term¹⁰. Reprinted with permission from Springer Nature. **C** Ray-inspired swimming biobot. i. cell alignment comparison between the actual ray (top) and the fabricated biobot (bottom) showing great similarity between the two. ii. Different muscle circuits with pre-programmed patterns of activation for sequential muscle activation. The design with dense serpentine traces has higher number of traveling waves. iii. The movement of the ray across the obstacles on its way depicting promising controllability and locomotion¹². Reprinted with permission from AAAS. Low-Reynold Swimmers: **(D)** i. a sperm-like micro biobot with the cell location near its head allowing movement of the system. ii. The movement of the system during the experiment shows bending and straightening¹¹. Reprinted with permission from Springer Nature. **E** magnetically controlled sperm bot⁵⁶. Reprinted with permission from John Wiley and Sons. **F** i. overall schematic of a neuromodulated microswimmer biobot. The idea is to penetrate the muscle ring with neurite outgrowth. iii. Two designs were created. One flagellum, and two flagella swimmers. iv. The results show that the system with 2 flagella was by far faster than its 1 flagellum counterpart¹⁸. Reprinted with permission from PNAS. **G** i. Biobot swimmer with curved tails highlighting the role of angular displacement of tails for propulsion. ii. location of motor neurons, muscle and ECM illustrating the actuation unit and its culture mechanism. iii. Diagram of the swimming position of the system⁵⁸. Reprinted with permission from AAAS. **H** Swimmer Jellyfish. (i) Swim controller (inactive) embedded into a free-swimming jellyfish. (ii) Square wave signal generated by the swim controller. (iii) Simplified schematics (Bottom) of *A. aurita* anatomy. (iv) *A. aurita* medusae were placed subumbrellar surface up for muscle stimulation experiments. (v) Schematic of vertical free-swimming experiments (vi) Swimming speeds and enhancement factors for 0, 0.25, 0.38, 0.50, 0.62, 0.75, 0.88, and 1.00 Hz swim controller frequencies. Scale bars, 1 cm [H (i)], 2 cm [H(iv)]. Reprinted with permission from AAAS⁷¹.



Control units for biohybrid robots usually means stimulating and starting the motion of the systems, but sometimes it can mean the opposite. The controlling/stimulating unit can act as a “brake” for the movement of the biobot. A research team came up with this idea and using this, they created a “floating-plane” that moves in the medium when the cardiac microtissues or “cellular engine” are relaxed and stops when the plane’s

wings bend. The working mechanism relies on applying Near Infrared Red (NIR) light which heats the hydrogel and causes shape change. The setup can be used for drug delivery to target cancer cells, moving freely and stopping to release the drug when the system reaches the cancer cells¹⁴.

Continuing the exploration of marine organisms, a ray-inspired biobot was engineered, aligning rat cardiac myocytes to mimic ray musculature

(Fig. 3C)¹². They investigated different muscle circuit designs, finding the intermediate serpentine structure provided the optimal balance between contraction control and efficient movement. This biobot demonstrated complex maneuverability over extended periods. In addition, it is noteworthy that a recent study introduced a hybrid design that combines both crawling and swimming modes, enabling these biohybrid robots to traverse terrestrial as well as aquatic environments⁵⁵.

In low Reynolds environment, A research team created a biohybrid flagellum: a spermatozoa-inspired system with an elastic filament with a stiff head, consisting of a small single cluster of contractile cells (Fig. 3D-i). The filament displacement sequence during a complete swimming cycle shows the functionality and locomotion of the system (Fig. 3D-ii)¹¹. The system introduced in this work was stimulated by magnetic control. In low Reynolds environment, bacteria-driven bots and sperm-bots have a vast number of research works dedicated to them. Another work in the similar area was conducted using a motile sperm cell and a cap in which the sperm cell would be trapped (Fig. 3E). The cap which is a rolled up microtube with incorporated magnetic layer, enables the directional control over the sperm cells using magnetic field⁵⁶.

Building up on this, a more recent work focused on developing a biocompatible drug delivery setup with these sperm cells as carriers of drug. Combining this with a magnetic microstructure enabled the system for controlled guidance and release at target sites. The sperms that were Doxorubicin(DOX)-loaded, could successfully reach the tumor cell apoptosis, and the system provided 87% of cell-killing within 72 h which is significant⁵⁷. An interesting approach in controlling the low Reynold swimmers is by introducing optogenetic motor neurons which was done in 2019. The idea was to create an actuation by light which was neuromuscular (Fig. 3F-i). The located neural cells in the proximity of the contractile muscle ring, and let the neural cells grow into the muscle ring making it light controllable (Fig. 3F-ii). They used optogenetic mouse Embryonic Stem Cells (ESCs) with PDMS structure. The moving part consisted of 1 leg in first platform, and 2 legs in the later (Fig. 3F-iii). The velocity comparison showed great superiority of the two-legged structure compared to the one-legged counterpart (Fig. 3F-iv)¹⁸.

Further using neurons in the swimming biobots' platforms, a low Reynold swimmer was developed using a novel PDMS structure design based on dual wavy tail (Fig. 3G-i) and C2C12 skeletal muscle rings. Motor neurons were added after 8 day in vitro (DIV8), to increase the amount of spontaneous twitching. It was found that the swimmers with neurons tend to show robust, spontaneous twitching on the order of $1.11 \pm 0.27\%$ the length of the muscle by day 8. On day 10, 4 out of 11 swimmers exhibited spontaneous twitching, while all 9 swimmers with neurons showed spontaneous twitching. On DIV8, the neurons and muscles were covered by ECM to protect them from drying out, both located on the PDMS structure (Fig. 3G-ii). Figure 3G-iii depicts the movement mechanism of this system. The swimming speed of this platform reached up to $86.8 \mu\text{m/s}$ ⁵⁸.

So far, different works used different control modalities which was decided based on their objective. Some used electrical stimulation^{41,59} as the means of control, others used optical stimulation (whether by introducing light sensitive proteins into the muscle cells^{60,61}, or using natural light sensitivity of components like fungal mycelia⁶²), and some utilized magnetic steering⁶³⁻⁶⁶. However, these are not the only stimulating techniques available. In 2011, a jellyfish-shaped micro-robot made of cardiomyocyte gel (a gel containing of cardiomyocyte which was cast in a mold to form the jellyfish shape) was introduced, which was controlled and moved chemically. They used epinephrine and nifedipine for increase and decrease of pulse frequency respectively⁶⁷. In a way, they could control the cardiac cell contracting units that are the least controllable among other contracting units like skeletal muscle cell which only contracts when it is stimulated.

In the field of swimming biomachines, when it comes to microswimmers, there is great room for creativity. One of these innovations is the use of bacterial chemotaxis as the control mechanism. The theory of bacterial chemotaxis is well established^{68,69}. It has been observed that positive temporal gradients of L-glutamate suppress the spontaneous directional

changes that *E.coli* bacteria exhibits in the absence of the stimulus. This result is in line with the model suggesting that the suppression of directional changes is proportional to the time rate of change of the fraction of chemoreceptors bound by attractant⁶⁹. One of the many works in this area used bacteria as the driving unit of their system, and chemotaxis (chemical control). The aim was to develop microswimmers that can navigate autonomously through chemotaxis, without the need of any external equipment. This work has the advantage of steering a large number of bots without external equipment. This work uses flagellated bacteria, like *Serratia marcescens* specifically for their chemotactic behaviors. Chemotaxis is a crucial characteristic for bacteria survival because chemotaxis guides them to nutrient sources and keeps them away from hazardous environments. The results of this study showed that bacterial chemotaxis can effectively control the microswimmer⁷⁰. This work has the potential to be applied for drug delivery in the future.

Enhancing the drug delivery capability which is one of the most notable uses of the biohybrid machines, An important research was conducted with the approach to create a biohybrid swimmer that uses both being driven by bacteria and double-emulsion microstructures to be used in transporting cargo, such as drugs, etc. In this study, bacteria-propelled microemulsions were observed to test swimming capabilities while being guided to cancer cells. These microswimmers reached the maximum velocity of $6.5 \mu\text{m/s}$, and successfully delivered the cargo with minimum toxicity⁷¹.

eBiobot swimmers

A biohybrid swimmer is created by researchers using onboard microelectronics on a living jellyfish³³. Compared to swimming naturally, this swimmer's equipment can swim three times faster. Additionally, compared to previous robots, this biobot can operate on 10–1000 times less electricity. The plan for controlled swimming in jellyfish is summed up in Fig. 3A. Bilateral electrodes were placed in the subumbrellar tissue, halfway between the center and bell border (Fig. 3H-i). Here, a portable, standalone micro-electric swim controller was developed that stimulates muscular contractions between 0.25 and 1.00 Hz by producing a square pulse wave with 3.7 V (Fig. 3H-ii). They devised a way to monitor the bell margin's motion in order to confirm that the swim controller could externally trigger jellyfish bell contractions. *A. aurita* medusae were injected with tags into the tissue and put subumbrellar surface up in a plate devoid of saltwater (Fig. 3H-iv). The swim controller let the animals to swim downhill at the following frequencies: 0.25, 0.38, 0.50, 0.62, 0.75, 0.88, and 1.00 Hz for experimental trials, and off (0 Hz) for control trials (Fig. 3H-v, vi). Future versions of the biohybrid robotic jellyfish can incorporate microelectronic sensors, enhance controllability, and utilize existing technology⁷².

Grippers

Biohybrid gripping robots have the capability to hold, manipulate, or move objects^{20,21,51}. By utilizing muscle tissue as actuators, these grippers can adapt their structure to grip objects with varying fragility, making them ideal for tasks requiring delicate handling. An interesting approach was done to control the contraction of gripping biohybrid robots. The idea was to use surface electromyography (EMG) signals, to signal the skeletal muscle cells of the gripper to contract or relax (Fig. 4A-i). The tissue engineered skeletal muscle was placed around the hook of the setup (Fig. 4A-ii) to alleviate the contraction. The formation of the tissue suggests that after 2 days, the tissue started to agglutinate around the anchors, and they kept the beam shape even after 45 days of culture (Fig. 4A-iii). In this work, they used PDMS as the bending structure²⁰.

In a research work, as a following work with biohybrid micropincers²¹, a micro pincer was created that was powered by DVT which is wrapped around the two notches of the gripper. The whole setup except the pincer tip including the DVT was placed in the medium (Fig. 4B-i) providing a biofriendly environment for the DVT. Studying the constraints of the structure, they measured the strain energy density distribution when relaxing and contracting in air (Fig. 4B-ii). While relaxing in the air, the gap between the tips of the gripper was 528 μm , and when contracting in the

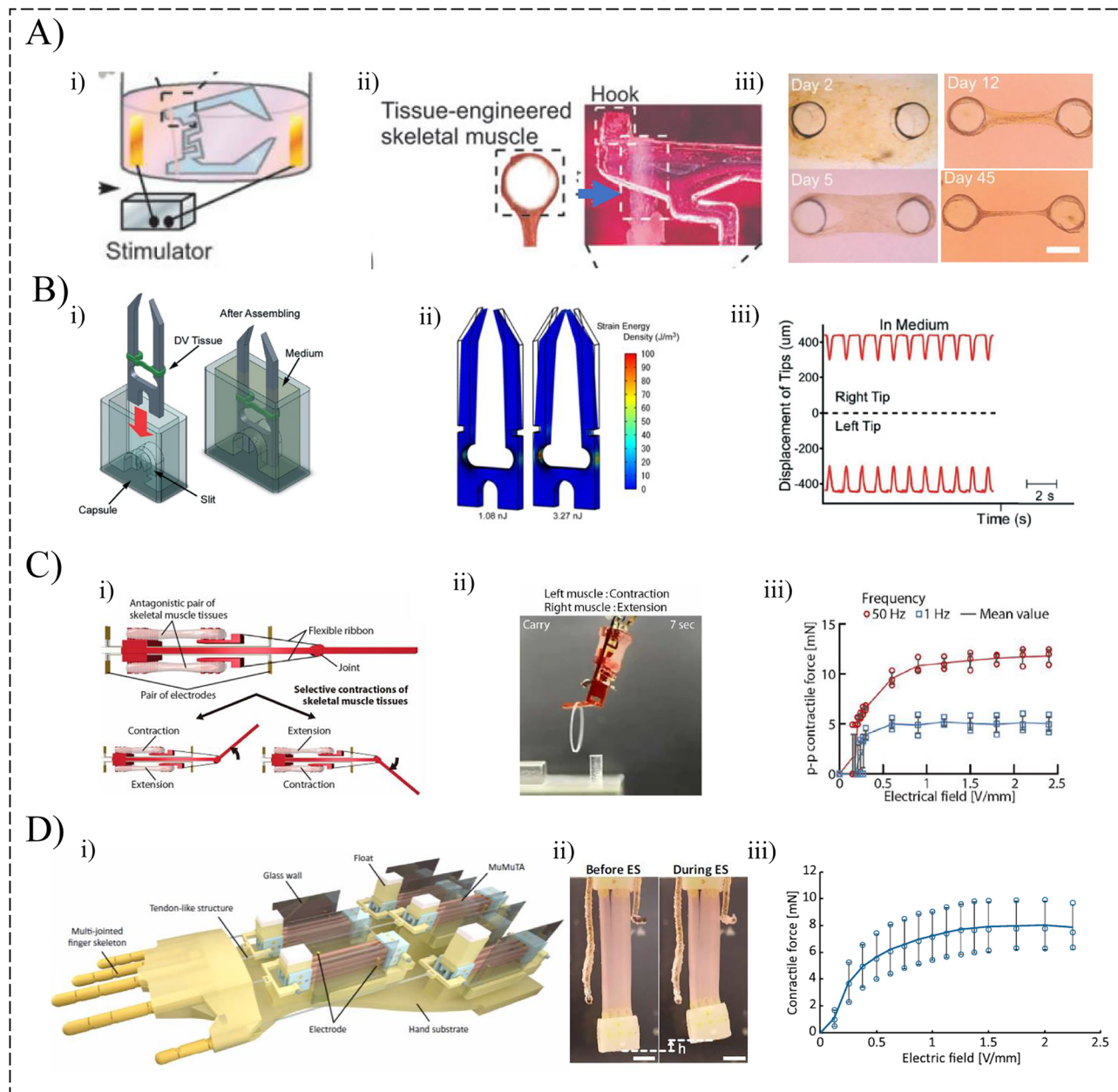


Fig. 4 | Gripping Biobots utilize muscle tissue or Dorsal Vein Tissue to contract and move the setup to manipulate objects. A i. The schematic of gripping system stimulated by electrical field which uses EMG signals taken from the hand of a subject to control the gripping mechanism. This system uses skeletal muscle tissue as the contracting unit. ii. The location of the skeletal muscle tissue on the gripper's structure which facilitates movement of the system. iii. tissue engineered skeletal muscle from day 2 to day 45 agglutinating around the anchor from day 2²⁰. Reprinted with permission from Mary Ann Liebert, Inc. B i. a gripping system in scale of millimeters using Dorsal Vein Tissue (DVT) ring as the contracting unit to make the arms get close to each other with contraction facilitating the gripping mechanism. ii.

The strain density distribution and total strain energy in air when relaxing(left) and when contracting(right). iii. Displacement the right and the left tip in medium²¹. Reprinted with permission from Royal Society of Chemistry. C i. An innovative gripping system with an antagonistic pair of muscle tissues to make the manipulating arms to move in two directions. ii. the gripper's performance showcasing its ability to hold ad pick up an object. iii. The contractile force of the tissues with respect to the electrical field with 1 Hz and 50 Hz of frequency¹⁹. Reprinted with permission from AAAS. D i. Illustration of the biohybrid hand. ii. before and after electrical stimulation (ES) of the MuMuTAs (scale bar, 5 mm). iii. Contractile force increasing with respect to electric field⁷³. Reprinted with permission from AAAS.

same environment, the gap was 180 μ m. The displacement of the tips with respect to time was also measured (Fig. 4B-iii)²¹.

One of the significant works in this area was conducted in 2018. A platform was created allowing for a pair of skeletal muscle tissues to work simultaneously with one tissue contracting and the other relaxing, the arm of this gripper can be moved in two directions, enhancing the manipulation capabilities (Fig. 4C-i). The contraction occurs when the electrical pulses are applied to the skeletal muscle tissues via parylene-coated gold electrodes located at both ends of the tissue. Each one of these two antagonistic tissues

have their own pair of electrodes. The relaxation happens when the electrical stimulation is stopped. This biobot can manipulate objects, hold them and pick them up while the arm is bending (Fig. 4C-ii). The contractile force of this system with respect to the electrical field showed that it has higher peak-peak contractile force in higher V/mm measures, furthermore, the frequency also plays a crucial role in the contractile force with 50 Hz of frequency showing much greater p-p contractile force than the 1 Hz showing greater strength of the gripping action when the frequency is higher (Fig. 4C-iii)¹⁹.

One of the latest works in the field of gripping biobots, is a biohybrid hand powered by multiple muscle tissue actuators (MuMuTAs) which produces high contractile force (~8mN). The system consists of multi-jointed finger skeletons, electrodes for stimulation of the muscles and hand substrate (Fig. 4D-i). Figure 4D-ii depicts the bending mechanism after electrical stimulation compared to before stimulation. The contractile force is also increased by increasing the electric field (Fig. 4D-iii). This interesting and novel setup achieved individual control of the fingers^{34,73}.

These setups however efficient and significant, still have limited bending range which limits their functionality. To improve the bending range of the biohybrid systems, an approach could be to use serially connected muscle rings, which can give large-scale bending motion⁵¹.

Pump bots

The heart, a natural muscular pump, plays a central role in circulating blood and maintaining physiological homeostasis. Inspired by this, various biohybrid pumping systems have been developed to mimic key cardiac functions. Two major parameters for evaluating pump performance are flow rate and pressure-volume (PV) loops. A common method for quantifying flow rate involves tracking the displacement of polystyrene microparticles suspended in fluid using high-speed imaging. PV loops, which reflect dynamic changes in intrachamber pressure and volume, are typically measured using conductance-based catheterization or microfluidic pressure-sensing systems. Below, we highlight several notable examples of advanced biohybrid pump systems.

Muscle-driven, impedance-based pump-bot. One representative system is an impedance-based pump-bot powered by engineered C2C12 skeletal muscle (Fig. 5A)³⁴. It consists of a stiff PDMS segment and a soft hydrogel tube, with a muscle ring positioned off-center around the soft region to induce asymmetric tube deformation (Fig. 5A-i, ii). This design generates unidirectional flow, achieving a flow rate of 11.62 $\mu\text{L}/\text{min}$ under spontaneous twitching and up to 22.68 $\mu\text{L}/\text{min}$ under electrical stimulation at 4 Hz (Fig. 5A-iii, iv). This pump-bot demonstrates the impressive flow output among current biohybrid systems, driven by skeletal muscle actuation.

Micro-spherical heart pump. Figure B shows a hollow PDMS sphere wrapped with a circular sheet of cardiomyocytes, which contract spontaneously to deform the chamber and drive pulsatile fluid flow³⁵. The resulting motion generates rhythmic flow through connected capillaries (Fig. 5B-i-iii), and particle tracking confirms unidirectional tracer displacement (Fig. 5B-iv). The estimated flow rate, assuming ideal valve conditions, is approximately 0.047 $\mu\text{L}/\text{min}$. This system represents one of the earliest and simplest cardiomyocyte-powered biohybrid pumps.

Engineered heart ventricle. This system demonstrates a three-dimensional ventricle fabricated from poly(ϵ -caprolactone) (PCL)/gelatin nanofiber structures seeded with aligned cardiomyocytes, including both neonatal rat ventricular myocytes (NRVMs) and human induced pluripotent stem cell-derived cardiomyocytes (hiPSC-CMs) as shown in Fig. 5C⁷⁴. The cells exhibit anisotropic alignment and layered infiltration across the surface and through the ventricular wall (C i, ii), resembling native myocardial architecture. PV loop measurements, obtained via catheterization in a custom bioreactor, reveal stroke work of $\sim 0.25 \text{ mmHg} \times \mu\text{L}$ for NRVMs and $0.05 \text{ mmHg} \times \mu\text{L}$ for hiPSC-CMs (C iii). The system is mounted in the bioreactor for real-time PV analysis and pharmacological testing, serving as a robust platform for cardiac disease modeling and drug evaluation under physiologically relevant conditions (Fig. 5C-iv).

Valved, cardiac-inspired minipump. A microfluidic miniPUMP integrates a helical structure seeded with hiPSC-CMs and features a passive suspension valve that opens and closes in response to pressure changes ($\sim 0.11\text{--}0.25 \text{ Pa}$), enabling a rectification ratio >0.80 below 2 Hz

(Fig. 5D-i)⁷⁵. The system replicates ventricular dynamics with a PV loop that includes distinct isovolumetric contraction and relaxation phases (Fig. 5D-ii). The measured loop demonstrates a peak systolic pressure of $\sim 42.8 \text{ Pa}$ and an ejection fraction of 4.1%, confirming effective chamber-based function under physiologic loading conditions. This platform is the first chip-scale biohybrid pump to recapitulate full ventricular mechanics, including isovolumetric phases.

From high-output skeletal muscle actuators to microfluidic platforms capable of reproducing full ventricular dynamics, each model addresses different aspects of physiological relevance, scalability, and controllability, advancing heart-on-a-chip technologies, disease modeling, pharmacological screening, and future biointegrated therapeutic devices.

Other types

The optobiobots are a type of biohybrid machines that rely significantly on light for detection^{13,15}. The detection-based optobots are engineered on the premise of color change that occurs due to the motion of cells which move the nanostructures, especially the periodic nanoridges causing the change in the reflection. These structures interact with light through a structural coloration phenomenon^{39,40,76}, meaning that the light wavelengths reflected from the surface only includes a subset of the wavelengths that was initially shined on it, i.e., the nanoridges on the wings control the propagation of photons³⁶⁻⁴⁰. So, when a biohybrid system works with this premise, it will be visible and detectable by the color change which is due to movement of the cells, and hence, change in the incident angle.

The detection-based optobots rely mainly on the surface structure. In this area a pair of Morpho butterfly wings actuated by engineered cardiac cells assembly were engineered. The cardiomyocytes were cultured on the wings and the autonomous contraction induce bending and color change. The change in color is due to nanostructure deformation. The result of their work under optical microscopy showed the structural color change of the wing with the cardiac cells cultured on. A single-cell-level detection illustrates the working concept. The relationship between the bending angles of the wing and the wavelength peak value in this paper's finding shows that more bending angle corresponds to lower reflected wavelengths¹³.

Another detectable optobiobot used a structural color layer for indicating the status of locomotion so when crawling by autonomous contraction of the cardiomyocytes as the actuation unit, on a filter paper, the changes in color were visible. Optical images also help better observe this during half myocardial cycle. The correlation between the bending angle and the reflection peak values showed the same relationship to that of the previous work on morpho butterfly wing¹⁵.

Table 1, compares the performance and design features of various biobots and complies key characteristics and performance metrics of representative biobots discussed.

Conclusion and future perspectives

Over the past decade, biobots have rapidly emerged at various scales by integrating living components with biomaterials. This innovative biohybrid approach has led to the development of motile biobots capable of walking, swimming, and grabbing. Early pioneering studies utilized muscle cells and tissue constructs for actuation, laying a solid foundation for more advanced biobots that mimic complex life-like movements. These initial biobots not only demonstrated the feasibility of combining biological systems with soft robotic systems, but also highlighted the vast potential for diverse applications. A notable example is the development of “pump-bots” in recent years, which leverage muscle contractions for fluid transport^{31,34,77}.

Despite this exciting progress, significant challenges remain for biobots to achieve widespread real-world applications. One of the primary obstacles is the longevity and stability of living cells. Ensuring the health and viability over extended periods is a persistent challenge, as cells are prone to degradation^{78,79}. Other challenges and limitations of this area include sensitivity of living contracting units to environmental factors and complicated requirements that currently exist in cell culture. Moreover, most of the current biobots are still constrained by their simple geometry and small

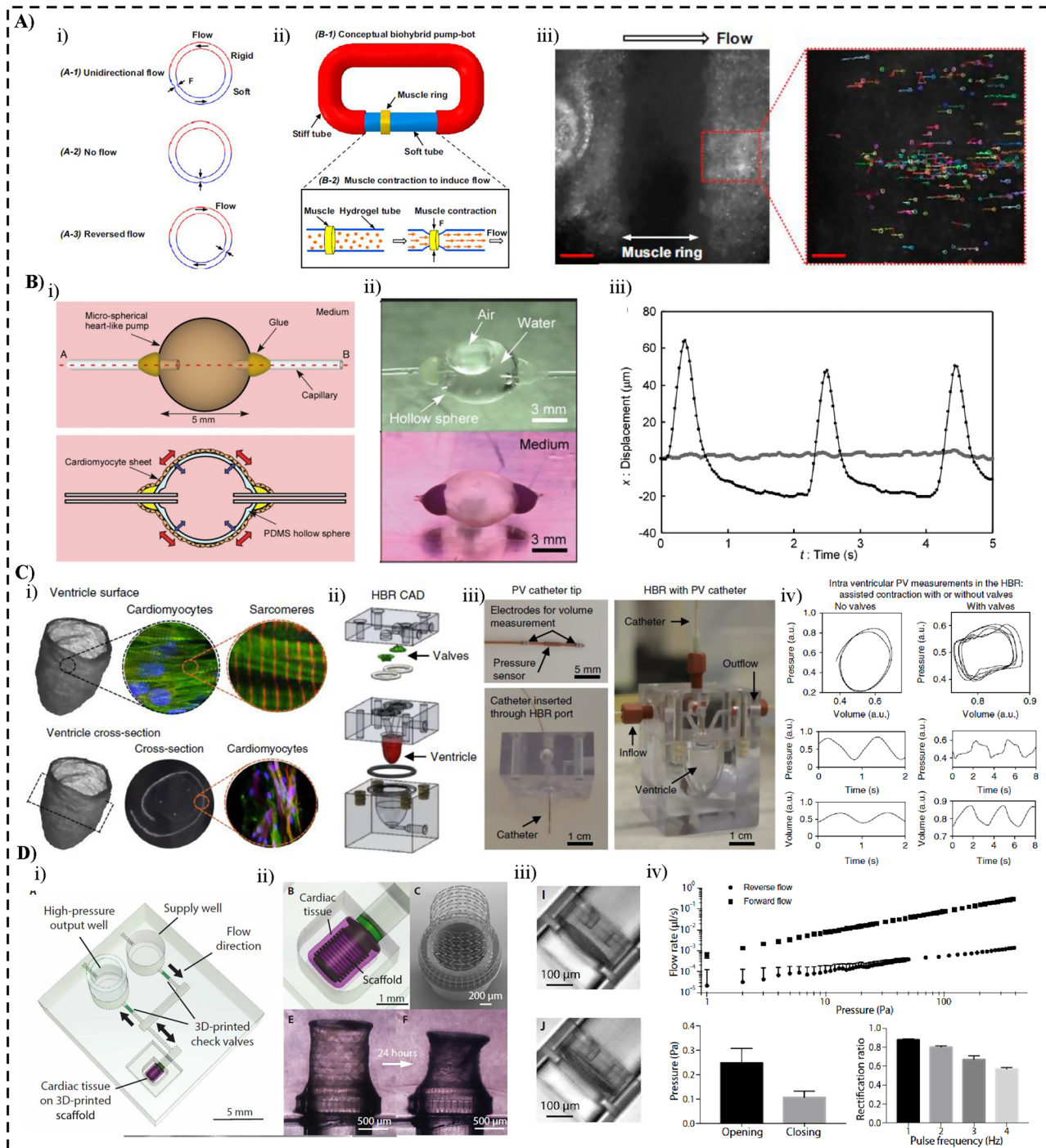


Fig. 5 | Pump bots. **A** Muscle-driven, impedance-based pump-bot: asymmetric tube deformation (i, ii) generates unidirectional flow (iii) with enhanced output under electrical stimulation (iv)³⁴. Reprinted from (34) with permission from PNAS. **B** Micro-spherical heart pump: a cardiomyocyte-wrapped PDMS sphere (i-iii) generates pulsatile flow through capillaries, with tracer displacement confirming rhythmic actuation (iv)³⁵. Reprinted from (35) with permission from Royal Society of Chemistry. **C** Engineered heart ventricle: (i-ii) Aligned cardiomyocytes and

layered infiltration on surface and cross-section. (iii) PV loops show contractile response to isoproterenol. (iv) Ventricle mounted in bioreactor for functional testing⁷⁴. Reprinted with permission from Springer Nature. **D** Valved, cardiac-inspired miniPUMP: (i) integrates a suspension valve for unidirectional flow, (ii) and (iii) reproduces ventricular-like mechanics with a pressure–volume loop showing isovolumetric phases (iv)⁷⁵. Reprinted with permission from AAAS.

actuation force, which greatly restrict their functionality and versatility for real world applications. Another key challenge lies in enhancing the control systems of biohybrid robots. Most existing systems still rely on external electrical or optical controls and lack the ability to perform complex tasks autonomously. A potential approach for addressing the challenges that this field faces regarding the biological units, can be the potential use of fungal mycelia as an alternative for the contracting sector of the biobots⁶².

A key trend in the field is the integration of microelectronics, neurons, and muscle tissues, paving the way for intelligent biobots capable of responding to environmental signals, adapting their actions, and even exhibiting basic learning and memory. Another area of significant progress is in the introduction of smart biomaterials (which can respond dynamically to external stimuli such as light, pH, temperature, or electric fields), and structural designs as advanced biobots structures. Advances in

Table 1 | Representative biohybrid robots grouped by locomotion type, with standardized entries for prototype, bioactuation type, operating modality, and performance metrics for clear comparison across categories

Biobot Prototype	Category	Bioactuation unit	Operating modality	Electronics	Force	Performance metrics	Control method	Ref
Muscular thin film robot	Walker, Gripper, pump, Swimmer	NRV/OMs	Wired	Pt wire electrodes	1–4 mN/mm ²	Walker: 0.13 mm/s Swimmer: 0.05 mm/s	Electrical	5
Caterpillar	Walker	Cardiomyocytes	NA	**	**	**	Chemical	12
Muscle strip crawler	Walker	Skeletal muscle tissue	NA	**	394.7 ± 56.5 μN	156.1 μm/s	Electrical	13
Walker 2016	Walker	C2C12	Wireless	**	Up to 300 μN	0.312 ± 0.016 mm/s	Electrical and Optical	14
Polypod microbot	Walker	Dorsal vessel tissue	NA	**	20 μN	3.5 μm/s	Autonomous, Electrical, Chemical	19
eBiobot	Walker	Skeletal muscle tissue	Wireless	Flexible circuit board, NFC chip, Microcontroller, RF antenna	737–1403 μN	0.83 mm/s	Optoelectrical	30
Junction bot	Walker	C2C12	Wired	RC pulse system, Pt electrodes	1.4 mN	>0.5 mm/s	Electrical	34
Low-Reynold swimmer	Swimmer	Cardiomyocytes	NA	**	1–10 μN	5–10 μm/s (1 tail) 81 μm/s (2 tails)	NA	8
Ray	Swimmer	Rat Cardiomyocytes	NA	**	**	3.2 mm/s	Optical	9
Floating-plane	Swimmer	Cardiomyocytes	NA	**	**	0.6 ± 0.2 mm/s	Optical	11
Neuromuscular Junction bot	Swimmer	C2C12+ optogenetic motor neurons	Wireless	**	**	0.7 μm/s	Optical	15
Neuromuscular eBiobot	Swimmer	Cardiomyocyte, motor neurons	Wireless	Flexible PCB, neural stimulation electrodes	**	0.73 mm/s	Electrical	31
Horizontal fish	Swimmer	Insect dorsal vessel tissue	Wireless	Transducer	42.7–79.6 μN	0.0117 mm/s	Autonomous	35
Magnet capped sperm-bot	Swimmer	Bovine Sperm	NA	**	**	0.01 mm/s	Magnetic	38
Microswimmer	Swimmer	Serratia marcescens	NA	**	0.5–3.0 pN	0.0024 mm/s	Magnetic	49
Chemical driven swimmer	Swimmer	Bacteria	NA	**	**	39.6 ± 12.9 μm/min	Chemical	52
Antagonistic Gripper	Gripper	Skeletal muscle tissue	Wired	Parylene-coated Au electrodes	Up to 0.3 mN	**	Electrical	16
Atmospheric Operable Gripper	Gripper	Insect dorsal vessel tissue	NA	**	19 μN	**	Electrical	18
Valveless pump	Pump	C2C12	Wired	**	**	**	Electrical	57
Adaptive pump bot	Pump	C2C12	Wired	**	**	**	Electrical	59

biomanufacturing^{80–82} are enabling the creation of smart biomaterials⁸³ and complex structures that allow for large-scale structural deformation and configuration, which will eventually enhance the biorobotic performance in locomotion tasks such as walking or swimming. These innovations will also facilitate the design of multifunctional biobots that can perform different types of locomotion, such as switching between crawling and swimming. Advanced microelectronics and biosensors are playing a crucial role in advancing biohybrid robotics, enabling more precise control and real-time monitoring of biobot systems. Bioelectronics (combination of biological specimen and electronic devices) enable remote control of movement, which is a critical step toward developing autonomous biobots capable of carrying out more complex tasks^{84,85}. Bioelectronics will also enable onboard computing, allowing biobots to process environmental signals independently. Integrated biosensors will allow biobots to respond adaptively to their surroundings⁸⁶, enabling novel applications that require high levels of environmental sensitivity and autonomy. For example, such systems would enable biobots to interpret real-time sensory data and adjust their behavior accordingly, which would be invaluable in applications like cancer-targeting drug delivery in the human body, where precision and adaptability are essential.

Biohybrid robotics holds promising potential in fields such as medicine^{87–89}, environmental science, and more others. One promising direction is the development of autonomous intelligent biobots with learning and memory capabilities. By incorporating bioelectronics and neuromuscular networks, future biobots could adjust their actions based on past experiences, making them capable of rudimentary decision-making. The *in vitro* biological neural networks (BNNs) can interact with the external world and perform preliminary intelligent behaviors like learning, memory and control^{90–92}. This adaptive behavior would be invaluable in scenarios requiring responsive, real-time interaction, such as targeted medical interventions or environmental sensing. The medical applications of biohybrid robots are particularly intriguing. For example, microrobots have been demonstrated as diagnostic and therapeutic agents capable of navigating complex biological environments to deliver therapeutics with precision⁹³. Beyond the biomedical domain, biohybrid swimmers and crawlers have been investigated as tools for environmental monitoring, where their ability to sense, adapt, and respond to dynamic conditions could be leveraged for detecting pollutants and ecological changes⁹⁴. Recent advances further highlight the potential of biohybrid robots in sustainability and monitoring applications. For example, Song et al.⁹⁴ demonstrated magnetotactic bacteria-based microrobots capable of coordinated 3D swarming for capturing aquatic micro- and nanoplastics. Similarly, Soliman et al.⁹⁵ introduced yeast-driven sensing robots that leverage yeast metabolism for environmental biosensing. Together, these studies underscore the expanding diversity of biological platforms and applications beyond traditional bacterial or mammalian systems.

In the future, biocompatible intelligent biobots could perform minimally invasive tasks within the human body. For example, a micro-bot could navigate in the circulatory system, reach a specific target site, and deliver therapeutic agents or perform localized repairs. This precision and functionality would mark a major advancement in personalized medicine and healthcare innovation⁶. However, these advances also raise novel ethical, legal, and regulatory challenges. For example, Mestre et al.⁹⁶ emphasize the need for dedicated governance frameworks to address the unique ethical issues of living robots.

Finally, interdisciplinary collaboration across materials science, synthetic biology, bioelectronics and biosensors, advanced manufacturing, and artificial intelligence and neural networks (for intelligent behavior) will drive the future of biohybrid robotics. The performance and capabilities of biohybrid robots are tightly linked to innovations in both biomaterials and bioengineering. By combining expertise from these diverse fields, researchers can develop biobots with enhanced durability, functionality, and autonomy, pushing the boundaries of what is possible in biohybrid systems. These interdisciplinary efforts will be the key to transforming biohybrid robotics from an emerging field into a practical technology, enabling a wide

range of real-world applications, from environmental monitoring to healthcare innovation.

In summary, biohybrid robotics represent an exciting frontier in biotechnology, where the integration of biology and engineering has the potential to revolutionize a wide range of fields. The creation of biohybrid motile robots- walkers, swimmers, grippers, pumps, optobots and eBiobots demonstrates the versatility and vast potential of these systems. As research progresses, biobots are set to redefine what is possible in robotics, paving the way for new advancements in medicine, environmental monitoring, and beyond.

Data availability

No datasets were generated or analysed during the current study.

Received: 14 November 2024; Accepted: 27 September 2025;

Published online: 09 December 2025

References

1. Pfeifer, R., Iida, F. & Bongard, J. New robotics: design principles for intelligent systems. *Artif. Life* **11**, 99–120 (2005).
2. Macenski, S., Foote, T., Gerkey, B., Lalancette, C. & Woodall, W. Robot operating system 2: design, architecture, and uses in the wild. *Sci. Robot.* **7**, eabm6074 (2022).
3. Doncieux, S., Bredeche, N., Mouret, J.-B. & Eiben, G., Ae. Evolutionary robotics: what, why, and where to. *Front. Robot. AI*. <https://doi.org/10.3389/frobt.2015.00004> (2015).
4. Wang, H., Mao, Y. & Du, J. Continuum robots and magnetic soft robots: from models to interdisciplinary challenges for medical applications. *Micromachines* **15**, 313 (2024).
5. Ricotti, L. et al. Biohybrid actuators for robotics: a review of devices actuated by living cells. *Sci. Robot.* **2**, eaaoq0495 (2017).
6. Zarepour, A., Khosravi, A., Iravani, S. & Zarrabi, A. Biohybrid micro/nanorobots: pioneering the next generation of medical technology. *Adv. Health. Mater.* **13**, e2402102 (2024).
7. Shepherd, R. F. et al. Multigait soft robot. *Proc. Natl. Acad. Sci. USA* **108**, 20400–20403 (2011).
8. George M. Whitesides, K. K. P. Muscular thin films for building actuators and powering devices. *Sci. Rep.* **317**, 1366–70 (2007).
9. Chan, V. et al. Development of miniaturized walking biological machines. *Sci. Rep.* **2**, 857 (2012).
10. Nawroth, J. C. et al. A tissue-engineered jellyfish with biomimetic propulsion. *Nat. Biotechnol.* **30**, 792–797 (2012).
11. Williams, B. J., Anand, S. V., Rajagopalan, J. & Saif, M. T. A self-propelled biohybrid swimmer at low Reynolds number. *Nat. Commun.* **5**, 3081 (2014).
12. Park, S. J. et al. Phototactic guidance of a tissue-engineered soft-robotic ray. *Science* **353**, 158–162 (2016).
13. Chen, Z. et al. Cardiomyocytes-actuated morpho butterfly wings. *Adv. Mater.* **31**, e1805431 (2019).
14. Xu, B. et al. A remotely controlled transformable soft robot based on engineered cardiac tissue construct. *Small* **15**, e1900006 (2019).
15. Sun, L., Chen, Z., Bian, F. & Zhao, Y. Bioinspired soft robotic caterpillar with cardiomyocyte drivers. *Adv. Funct. Mater.* **30**, 1907820 (2019).
16. Cvetkovic, C. et al. Three-dimensionally printed biological machines powered by skeletal muscle. *Proc. Natl. Acad. Sci. USA* **111**, 10125–10130 (2014).
17. Raman, R. et al. Optogenetic skeletal muscle-powered adaptive biological machines. *Proc. Natl. Acad. Sci. USA* **113**, 3497–3502 (2016).
18. Aydin, O. et al. Neuromuscular actuation of biohybrid motile bots. *Proc. Natl. Acad. Sci. USA* **116**, 19841–19847 (2019).
19. Morimoto, Y., Onoe, H. & Takeuchi, S. Biohybrid robot powered by an antagonistic pair of skeletal muscle tissues. *Sci. Robot.* **3**, eaat4440 (2018).

20. Kabumoto, K., Hoshino, T., Akiyama, Y. & Morishima, K. Voluntary movement controlled by the surface EMG signal for tissue-engineered skeletal muscle on a gripping tool. *Tissue Eng. Part A* **19**, 1695–1703 (2013).
21. Akiyama, Y. et al. Atmospheric-operable bioactuator powered by insect muscle packaged with medium. *Lab Chip* **13**, 4870–4880 (2013).
22. Akiyama, Y., Hoshino, T., Iwabuchi, K. & Morishima, K. Room temperature operable autonomously moving bio-microrobot powered by insect dorsal vessel tissue. *PLoS ONE* **7**, e38274 (2012).
23. Akiyama, Y. et al. Rapidly-moving insect muscle-powered microrobot and its chemical acceleration. *Biomed. Microdevices* **14**, 979–986 (2012).
24. Jo, B., Motoi, K., Morimoto, Y. & Takeuchi, S. Dynamic and static workout of in vitro skeletal muscle tissue through a weight training device. *Adv. Health. Mater.* **13**, e2401844 (2024).
25. Glancy, B. & Balaban, R. S. Energy metabolism design of the striated muscle cell. *Physiol. Rev.* **101**, 1561–1607 (2021).
26. Einfalt, T. et al. Biomimetic artificial organelles with in vitro and in vivo activity triggered by reduction in microenvironment. *Nat. Commun.* **9**, 1–12 (2018).
27. Sleath, H., Mognetti, B., Elani, Y. & Di Michele, L. Chemotactic crawling of multivalent vesicles along ligand-density gradients. *arXiv* <https://doi.org/10.48550/arXiv.2310.09990> (2023).
28. Wang, J., Wang, Y., Kim, Y., Yu, T. & Bashir, R. Multi-actuator light-controlled biological robots. *APL Bioeng.* **6**, 036103 (2022).
29. Wang, J. et al. Computationally assisted design and selection of maneuverable biological walking machines. *Adv. Intell. Syst.* **3**, 2000237 (2021).
30. Yamatsuta, E., Ping Beh, S., Uesugi, K., Tsujimura, H. & Morishima, K. A micro peristaltic pump using an optically controllable bioactuator. *Engineering* **5**, 580–585 (2019).
31. Li, Z. & Saif, M. T. A. Mechanics of biohybrid valveless pump-bot. *J. Appl. Mech.* **88**, 111004 (2021).
32. Rajewicz, W. et al. Organisms as sensors in biohybrid entities as a novel tool for in-field aquatic monitoring. *Bioinspir. Biomim.* **19**, 015001 (2024).
33. Shoji, K., Morishima, K., Akiyama, Y., Nakamura, N. & Ohno, H. in *IEEE International Conference on Mechatronics and Automation* 629–634 (IEEE, 2016).
34. Li, Z. et al. Biohybrid valveless pump-bot powered by engineered skeletal muscle. *Proc. Natl. Acad. Sci. USA* **116**, 1543–1548 (2019).
35. Tanaka, Y. et al. A micro-spherical heart pump powered by cultured cardiomyocytes. *Lab Chip* **7**, 207–212 (2007).
36. Vukusic, P. & Sambles, J. R. Photonic structures in biology. *Nature* **424**, 852–855 (2003).
37. Kinoshita, S., Yoshioka, S. & Miyazaki, J. Physics of structural colors. *Rep. Prog. Phys.* **71**, 076401 (2008).
38. Sato, O., Kubo, S. & Gu, Z.-Z. Structural color films with lotus effects, superhydrophilicity, and tunable stop-bands. *Acc. Chem. Res.* **42**, 1–10 (2009).
39. Butt, H. et al. Morpho butterflies: morpho butterfly-inspired nanostructures (Advanced Optical Materials 4/2016). *Adv. Opt. Mater.* **4**, 489–489 (2016).
40. Giraldo, M., Yoshioka, S., Liu, C. & Stavenga, D. Coloration mechanisms and phylogeny of morpho butterflies. *J. Exp. Biol.* **219**, 3936–3944 (2016).
41. Kim, Y. et al. Remote control of muscle-driven miniature robots with battery-free wireless optoelectronics. *Sci. Robot.* **8**, eadd1053 (2023).
42. Tetsuka, H., Gobbi, S., Hatanaka, T., Pirrami, L. & Shin, S. R. Wirelessly steerable bioelectronic neuromuscular robots adapting neurocardiac junctions. *Sci. Robot.* **9**, eado0051 (2024).
43. Webster-Wood, V. A. et al. Biohybrid robots: Recent progress, challenges, and perspectives. *Bioinspiration Biomim.* **18**, 015001 (2022).
44. Mestre, R., Patiño, T. & Sánchez, S. Biohybrid robotics: From the nanoscale to the macroscale. *WIREs Nanomed. Nanobiotechnol.* **13**, e1703 (2021).
45. Sun, L. et al. Biohybrid robotics with living cell actuation. *Chem. Soc. Rev.* **49**, 4043–4069 (2020).
46. Li, T. & Takeuchi, S. Advancing biohybrid robotics: innovations in contraction models, control techniques, and applications. *Biophys. Rev.* **6**, 011304 (2025).
47. Kim, J. et al. Establishment of a fabrication method for a long-term actuated hybrid cell robot. *Lab. Chip.* **7**, 1504–1508 (2007).
48. Gao, L. et al. A muscle-machine hybrid crawler: omnidirectional maneuverability and high load capacity. *Sens. Actuators B. Chem.* **393**, 134333 (2023).
49. Pagan-Diaz, G. J. et al. Simulation and Fabrication of Stronger, Larger, and Faster Walking Biohybrid Machines. *Adv. Funct. Mater.* **28**, 1801145 (2018).
50. Yoon, J., Eyster, T. W., Misra, A. C. & Lahann, J. Cardiomyocyte-Driven Actuation in Biohybrid Microcylinders. *Adv. Mater.* **27**, 4509–4515 (2015).
51. Morita, T., Nie, M. & Takeuchi, S. in *IEEE 37th International Conference on Micro Electro Mechanical Systems (MEMS)*, 267–268 (IEEE, 2024).
52. Kinjo, R., Morimoto, Y., Jo, B. & Takeuchi, S. Biohybrid bipedal robot powered by skeletal muscle tissue. *Matter* **7**, 948–962 (2024).
53. Yalikun, Y. et al. Insect muscular tissue-powered swimming robot. *Actuators* **8**, 30 (2019).
54. Lee, K. Y. et al. An autonomously swimming biohybrid fish designed with human cardiac biophysics. *Science* **375**, 639–647 (2022).
55. Kim, D., Shin, M., Choi, J.-H. & Choi, J.-W. Actuation-augmented biohybrid robot by hyaluronic acid-modified au nanoparticles in muscle bundles to evaluate drug effects. *ACS Sens.* **7**, 740–747 (2022).
56. Magdanz, V., Sanchez, S. & Schmidt, O. G. Development of a sperm-flagella driven micro-bio-robot. *Adv. Mater.* **25**, 6581–6588 (2013).
57. Xu, H. et al. Sperm-hybrid micromotor for targeted drug delivery. *ACS Nano* **12**, 327–337 (2018).
58. Drennan, W. C. et al. A forward-engineered, muscle-driven soft robotic swimmer. *Sci. Adv.* **11**, eadu8634 (2025).
59. Smith, A. S. et al. A multiplexed chip-based assay system for investigating the functional development of human skeletal myotubes in vitro. *J. Biotechnol.* **185**, 15–18 (2014).
60. Raman, R. et al. Damage, healing, and remodeling in optogenetic skeletal muscle bioactuators. *Adv. Healthc Mater.* **6**, 10.1002/adhm.201700030 (2017).
61. Vizsnyiczai, G. et al. Light controlled 3D micromotors powered by bacteria. *Nat. Commun.* **8**, 15974 (2017).
62. Mishra, A. K. et al. Sensorimotor control of robots mediated by electrophysiological measurements of fungal mycelia. *Sci. Robot.* **9**, eadk8019 (2024).
63. Yasa, O., Erkoc, P., Alapan, Y. & Sitti, M. Microalga-powered microswimmers toward active cargo delivery. *Adv. Mater.* **30**, e1804130 (2018).
64. Shi, X., Shi, Z., Wang, D., Ullah, M. W. & Yang, G. Microbial cells with a Fe(3) O(4) doped hydrogel extracellular matrix: manipulation of living cells by magnetic stimulus. *Macromol. Biosci.* **16**, 1506–1514 (2016).
65. Carlsen, R. W., Edwards, M. R., Zhuang, J., Pacoret, C. & Sitti, M. Magnetic steering control of multi-cellular bio-hybrid microswimmers. *Lab Chip* **14**, 3850–3859 (2014).
66. Khalil, I. S. M., Magdanz, V., Sanchez, S., Schmidt, O. G. & Misra, S. Biocompatible, accurate, and fully autonomous: a sperm-driven micro-bio-robot. *J. Micro-Bio Robot.* **9**, 79–86 (2014).
67. Takemura, R., Akiyama, Y., Hoshino, T. & Morishima, K. In *16th International Solid-State Sensors, Actuators and Microsystems Conference*, 2442–2445 (IEEE, 2011).
68. Berg, H. C. & Brown, D. A. Chemotaxis in escherichia coli analysed by three-dimensional tracking. *Nature* **239**, 500–504 (1972).

69. Brown, D. A. & Berg, H. C. Temporal stimulation of chemotaxis in *Escherichia coli*. *Proc. Natl. Acad. Sci. USA* **71**, 1388–1392 (1974).

70. Zhuang, J. & Sitti, M. Chemotaxis of bio-hybrid multiple bacteria-driven microswimmers. *Sci. Rep.* **6**, 32135 (2016).

71. Singh, A. V., Hosseiniidoust, Z., Park, B.-W., Yasa, O. & Sitti, M. Microemulsion-based soft bacteria-driven microswimmers for active cargo delivery. *ACS Nano* **11**, 9759–9769 (2017).

72. Xu, N. W. & Dabiri, J. O. Low-power microelectronics embedded in live jellyfish enhance propulsion. *Sci. Adv.* **6**, eaaz3194 (2020).

73. Ren, X., Morimoto, Y. & Takeuchi, S. Biohybrid hand actuated by multiple human muscle tissues. *Sci. Robot* **10**, eadr5512 (2025).

74. MacQueen, L. A. et al. A tissue-engineered scale model of the heart ventricle. *Nat. Biomed. Eng.* **2**, 930–941 (2018).

75. Michas, C. et al. Engineering a living cardiac pump on a chip using high-precision fabrication. *Sci. Adv.* **8**, eabm3791 (2022).

76. Smith, G. S. Structural color of Morpho butterflies. *Am. J. Phys.* **77**, 1010–1019 (2009).

77. Li, Z. et al. Adaptive biohybrid pumping machine with flow loop feedback. *Biofabrication* <https://doi.org/10.1088/1758-5090/ac4d19> (2022).

78. Cvetkovic, C. et al. Investigating the life expectancy and proteolytic degradation of engineered skeletal muscle biological machines. *Sci. Rep.* **7**, 3775 (2017).

79. Anand, S. V., Ali, M. Y. & Saif, M. T. A. Cell culture on microfabricated one-dimensional polymeric structures for bio-actuator and bio-bot applications. *Lab a Chip* **15**, 1879–1888 (2015).

80. Onoe, H. et al. Metre-long cell-laden microfibres exhibit tissue morphologies and functions. *Nat. Ure Mater.* **12**, 584–590 (2013).

81. Ahrens, J. H. et al. Programming cellular alignment in engineered cardiac tissue via bioprinting anisotropic organ building blocks. *Adv. Mater.* **34**, e2200217 (2022).

82. Chang, S. Y., Lee, J. Z. W., Ranganath, A. S., Ching, T. & Hashimoto, M. Poly(ethylene-glycol)-dimethacrylate (PEGDMA) composite for stereolithographic bioprinting. *Macromol. Mater. Eng.* **309**, 2400143 (2024).

83. Yoshida, K., Kohno, K., Hiratsuka, Y. & Onoe, H. Macroscale collagen-actomyosin hybrid actuator built from bioderived materials. *Adv. Funct. Mater.* **33**, 2307766 (2023).

84. Wehner, M. et al. An integrated design and fabrication strategy for entirely soft, autonomous robots. *Nature* **536**, 451–455 (2016).

85. Yoshida, K. & Onoe, H. Soft spiral-shaped microswimmers for autonomous swimming control by detecting surrounding environments. *Adv. Intell. Syst.* **2**, 2000095 (2020).

86. Yamada, T. et al. Highly sensitive VOC detectors using insect olfactory receptors reconstituted into lipid bilayers. *Sci. Adv.* **7**, eabd2013 (2021).

87. Seyed, S. M. R., Asoodeh, A. & Darroudi, M. The human immune cell simulated anti-breast cancer nanorobot: the efficient, traceable, and dirigible anticancer bio-bot. *Cancer Nanotechnol.* **13**, 44 (2022).

88. Huska, D., Mayorga-Martinez, C. C., Zelinka, R. & Pumera, M. Magnetic biohybrid robots as efficient drug carrier to generate plant cell clones. *Small* **18**, 2200208 (2022).

89. Panda, V., Saindane, A. & Pandey, A. Nanobots: revolutionising the next generation of biomedical technology and drug therapy. *Curr. Drug Ther.* **19**, 403–412 (2024).

90. Chen, Z. et al. An overview of in vitro biological neural networks for robot intelligence. *Cyborg. Bionic. Syst.* **4**, 0001 (2023).

91. Touchstone, L. A. *Microelectronics Give Researchers a Remote Control for Biological Robots*. <https://news.illinois.edu/view/6367-401079005#image-4> (2023).

92. Raman, R., Cvetkovic, C. & Bashir, R. A modular approach to the design, fabrication, and characterization of muscle-powered biological machines. *Nat. Protoc.* **12**, 519–533 (2017).

93. SciTechDaily. *Microscopic Biohybrid Robots Propelled by Muscles & Nerves Built by Researchers*. <https://scitechdaily.com/microscopic-biohybrid-robots-propelled-by-muscles-nerves-built-by-researchers/> (2024).

94. Song, S.-J. et al. Precisely navigated biobot swarms of bacteria *magnetospirillum magneticum* for water decontamination. *ACS Appl. Mater. Interfaces* **15**, 7023–7029 (2023).

95. Soliman, M., Forbes, F. & Damian, D. D. Yeast-driven and bioimpedance-sensitive biohybrid soft robots. *Cyborg Bionic. Syst.* <https://doi.org/10.34133/cbsystems.02> (2025).

96. Mestre, R., Astobiza, A. M., Webster-Wood, V. A., Ryan, M. & Saif, M. T. A. Ethics and responsibility in biohybrid robotics research. *Proc. Natl. Acad. Sci. USA* **121**, e2310458121 (2024).

Acknowledgements

Z.L. acknowledges the support from the Presidential Frontier Faculty Fellow Start-Up Funding, High Priority Area Research Seed Grant, and Drug Discovery Institute (DDI) Seed Grant from the University of Houston. This work was also supported by the National Institute of Biomedical Imaging and Bioengineering of the National Institutes of Health under Award Number R21EB037317.

Author contributions

Z.L. planned and conceptualized the paper, provided supervision, guidance, and funding, and led the preparation of the paper. A.G., with the assistance of A.K.T. and C.L. conducted the literature survey, wrote the original draft and created the figures and tables. All authors read and edited the paper.

Competing interests

The authors declare no competing interests.

Additional information

Correspondence and requests for materials should be addressed to Zhengwei Li.

Reprints and permissions information is available at <http://www.nature.com/reprints>

Publisher's note Springer Nature remains neutral with regard to jurisdictional claims in published maps and institutional affiliations.

Open Access This article is licensed under a Creative Commons Attribution-NonCommercial-NoDerivatives 4.0 International License, which permits any non-commercial use, sharing, distribution and reproduction in any medium or format, as long as you give appropriate credit to the original author(s) and the source, provide a link to the Creative Commons licence, and indicate if you modified the licensed material. You do not have permission under this licence to share adapted material derived from this article or parts of it. The images or other third party material in this article are included in the article's Creative Commons licence, unless indicated otherwise in a credit line to the material. If material is not included in the article's Creative Commons licence and your intended use is not permitted by statutory regulation or exceeds the permitted use, you will need to obtain permission directly from the copyright holder. To view a copy of this licence, visit <http://creativecommons.org/licenses/by-nc-nd/4.0/>.

© The Author(s) 2025